ARCHIVES OF TRANSPORT *ISSN (print):* *0866-9546*
Volume 39, Issue 3, 2016 *e-ISSN (online):* *2300-8830*
DOI: 10.5604/08669546.1225448

THE USE OF A LINEAR HALF-VEHICLE MODEL FOR THE OPTIMIZATION OF DAMPING IN THE PASSIVE SUSPENSION SYSTEM OF A RAILWAY CAR

Zbigniew Lozia[1,2], Ewa Kardas-Cinal[3]
[1,3]Warsaw University of Technology, Faculty of Transport, Warsaw, Poland
[2]Automotive Industry Institute PIMOT, Poland
[1]e-mail: lozia@wt.pw.edu.pl
[3]e-mail: ekc@wt.pw.edu.pl

Abstract: *The paper presents a methodology of optimizing the parameters of the passive suspension system of a railway vehicle. A linear half-vehicle model and an example of the procedure carried out to optimize a selected parameter of the model have been demonstrated. A method of the selection of damping in the suspension system of a railway vehicle, based on over 40-year achievements of the cited authors of publications in the field of motor vehicles, has been shown. The optimization of linear damping in the secondary suspension system of a passenger carriage moving on a track with random profile irregularities has been described in detail. The algorithms adopted for the calculations have a wider range of applicability; especially, they may be used for determining the optimum values of the other parameters of the railway vehicle model under analysis, i.e. stiffness of the secondary suspension system as well as stiffness and damping of the primary suspension system.*

Key words: *suspension system of a railway vehicle, damping coefficient, optimization, half-vehicle model.*

1. Introduction and references to the literature

In vehicle dynamics, a special branch is discerned, where the vehicle motion in the vertical direction is described and analysed. It is chiefly dedicated to the translational vibrations, but angular vibrations in the vertical planes parallel and perpendicular to the vehicle symmetry plane are addressed as well. In simplified analyses, "half-vehicle" and "quarter-vehicle" models are used. This is chiefly applicable to motor vehicles (Arczyński, 1993; Crolla, 1996; Firth, 1991; Gobbi et al., 2006; Gobbi & Mastinu, 2001; Kamiński & Pokorski, 1983; Kasprzyk & Prochowski, 1990; Kasprzyk et al., 1974; Lozia, 1985; Lozia, 2016; Mitschke, 1989; Mitschke, 1977; Muluka, 1998; Patil & Joshi, 2014; Otenberg, 1974; Ryba, 1974; Sekulić & Devidović, 2011; Sharp & Crolla, 1987; Sharp & Hassan, 1986; Ślaski, 2012; Verros et al., 2005; Yi & Song, 1999; Wong, 2001), but works where such models were used for the research on the railway vehicle motion can be indicated as well (Grzyb & Bogacz, 2015; Liang et al., 2012; O'Brien et al., 2015; Sim et al., 2013).

Models of this type, used for works on motor vehicles, appeared in 1970s (eg. Kasprzyk & Prochowski, 1990; Mitschke, 1977; Otenberg, 1974; Ryba, 1974). They were utilized in many publications of 1980s (e.g. Kamiński & Pokorski, 1983; Lozia, 1985; Mitschke, 1977; Sharp & Crolla, 1987; Sharp & Hassan, 1986) and 1990s (e.g. Firth, 1991; Kasprzyk & Prochowski, 1990, Muluka, 1998). In the 21st century, they are still useful for more complex and comprehensive analyses, including the works where the results are synthesized in the form of recommendations for vehicle designers (e.g. Gobbi et al., 2006; Gobbi & Mastinu, 2001; Konieczny, 2011; Patil & Joshi, 2014; Sekulić & Devidović, 2011; Ślaski, 2012; Verros et al., 2005; Wong, 2001). Such models are both linear and non-linear and represent passive, semi-active, and active suspension systems. In some of the works, the model tests are supplemented by experiments carried out on systems whose structure is close to that of the quarter-vehicle model (Konieczny, 2011; Patil & Joshi, 2014; Ślaski, 2012). At present, models of this type are used in sophisticated optimizing algorithms, including those dedicated to searching for Pareto-optimal solutions (Kwarciński, 2007), where the random nature of selected model parameters (sprung mass determined by hardly-predictable vehicle load and tyre stiffness depending on inflation pressure, which varies during

the vehicle operation, e.g. Gobbi et al. (2006)), is taken into account, or where designs of variable-damping, semi-active, and active suspension systems are assessed (e.g. Crolla, 1996;Firth, 1991; Gobbi et al., 2006; Gobbi & Mastinu, 2001; Sekulić & Devidović, 2011; Sharp & Crolla, 1987; Sharp & Hassan, 1986; Ślaski, 2012; Verros et al., 2005; Wong, 2001).

In the research works on railway vehicles, the simplified quarter-vehicle models are chiefly used to analyse the variable-damping suspension system. In such an application, models of this type were used to investigate the vertical vehicle dynamics (Grzyb & Bogacz, 2015; Li & Goodall, 1999; Liang et al., 2012), as it is in the case of motor vehicles, and the lateral vehicle dynamics related to the limitation of the position of wheels moving on a track (Sim et al., 2013). In such models, track profile irregularities (vertical and lateral) are represented, which define the kinematic excitation that results in vehicle body vibrations. A quarter-vehicle model was also used in O'Brien et al. (2015) for numerical validation of the method that was there proposed for determining the vertical irregularities in the track profile on the grounds of measurements of bogie acceleration; methods of this kind are employed as an inexpensive alternative to the standard measurements of track geometry with the use of laser systems installed in track inspection cars.

At the initial stage, the works on vehicle dynamics were seriously limited by the analysis and calculation methods available. It was as late as in 1950s that mathematical methods began to be used, thanks to which analytical considerations with limited computational potential became possible. The introduction of computer-based techniques and new methods of examining linear and non-linear mechanical systems with deterministic or random excitation has made it possible to carry out calculations that would be more extensive, with simple or more complex mathematical models being used. Particularly important here are monograph-like works, which provide a basis for building models with different complexity degree and for analysing their properties. For the authors from Western Europe and North America, this chiefly applies to the works by Meirovitch (1975), Newland (1984), Mitschke (1977, 1989), Wong (2001), Kalker (1982) and Wickens (1976). In Poland, considerable importance is also attached, apart from the above, to the works by Rotenberg (1974), Kamiński & Pokorski (1983), Osiecki (1979, 1994), Osiecki et al. (2006), Kasprzyk & Prochowski, 1990 and Kasprzyk et al. (1974). The first publications backed up with extensive computer calculation results appeared as recently as in 1970s. Such works have been continued until now and they cover a wide spectrum of issues related to vehicle dynamics. In the field of railway vehicles, the works considered to be of considerable importance are e.g. those described in publications by Chudzikiewicz (1995), Choromański and Zboiński (1991), Zboiński (2000, 2004) and Piotrowski (1990) as well as in a monograph edited by Kisilowski (1991).

In this study, over 40-year achievements of many foreign and Polish authors in the field of methods of optimizing the characteristics of passive vehicle wheel suspension systems have been utilized. The railway vehicle dynamics has been analysed with taking as a reference the works in the field of the dynamics of motor vehicles (Arczyński, 1993; Kamiński & Pokorski, 1983; Lozia, 2016; Mitschke, 1989; Mitschke, 1977; Osiecki, 1994; Otenberg, 1974; Wong, 2001). The optimization of linear damping in the secondary suspension system in a simple model of a railway vehicle moving on an uneven track with random vertical irregularities has been described in detail in the subsequent part of this paper.

The authors of an overwhelming majority of the publications where the said optimization problem is addressed enumerate three main assessment criteria, which are related to the minimization of the driver and passengers' discomfort measures as well as to changes in the normal reaction at the tyre-road contact and to reduction in the range of working displacements of the suspension system (Crolla, 1996; Firth, 1991; Gobbi et al., 2006; Gobbi & Mastinu, 2001; Kasprzyk & Prochowski, 1990, Kasprzyk et al., 1974; Mitschke, 1989; Mitschke, 1977; Muluka, 1998; Orvnäs, 2010; Orvnäs, 2011; Otenberg, 1974; Ryba, 1974; Sekulić & Devidović, 2011; Sharp & Crolla, 1987; Sharp & Hassan, 1986; Ślaski, 2012; Verros et al., 2005; Wong, 2001). In Sharp & Crolla (1987), the previous works (carried out by 1987) on the influence of damping in the suspension system on the measures of discomfort and safety hazard of a motor vehicle have been summed up. A contradiction between the existing requirements has

been highlighted. Increased damping in the suspension system impairs the comfort but improves the safety. The results presented in the publications referred to above also show that a growth in the damping is accompanied by a reduction in the range of working displacements of the suspension system. Most of the authors of the publications quoted here assume that the excitation is a Gaussian stationary random process in the domain of wavelength L [m], wave number (spatial frequency) 1/L [1/m], or angular (spatial) frequency of the road profile $\Omega = 2\pi/L$ [rad/m]. The frequency band of the vibrations of bodies constituting the vehicle model is determined. It is limited in consideration of the properties of the object under test or the problem being analysed (ride comfort, wheel-ground interaction, etc.). In the publications quoted, different frequency bands were chosen, predominantly 0-20 Hz (Muluka, 1998, Verros et al., 2005), 0-25 Hz or 0-30 Hz (Mitschke, 1989; Mitschke, 1977; Ślaski, 2012) or 1-80 Hz (Ślaski, 2012). An important limitation of the analyses, which are carried out for frequencies of up to 80 Hz, arises from the fact that in the ISO standards concerning the vibrational comfort (ISO 2631–1, 1985 & 1997), the acceptability limits are specified for a frequency band of 0-80 Hz.

2. General description of the half-vehicle model

The model of a railway vehicle (Figs. 1a and 1b) represents a conventional passenger carriage seated on two-axle bogies, model 25ANa (Kardas-Cinal, 2013). The primary physical model of the vehicle consists of 7 rigid bodies representing vehicle body, two bogies, and four wheelsets. The model has 27 degrees of freedom, which correspond to the lateral, vertical, and angular displacements of the bodies that make up the complete vehicle. The model represents a railway vehicle moving on a straight track with random profile irregularities. The positions of the railway vehicle component bodies are described in a moving reference frame Oxyz attached to the centreline of the track of nominal dimensions. The origin O of the reference coordinate system is situated in the track centreline and moves along the centreline with a velocity equal to vehicle speed v. The coordinate axis Ox is tangent to the centreline of the track with the nominal dimensions (which is ideally straight), the coordinate axis Oz is pointing vertically downwards, and the coordinate axis Oy, perpendicular to the other axes (Ox and Oz), is directed horizontally from the left rail to the right one. The moving reference frame Oxyz is an inertial frame because the railway vehicle moves along the straight track with a constant speed v. The position of the k^{th} body in the vehicle model is described by six coordinates, i.e. coordinates x_k, y_k, and z_k of the centre of mass of the body and three angles φ_k, ψ_k, and θ_k, which define the orientation of the body in the space. These angles are referred to as follows: φ_k is the pitch angle, ψ_k is the yaw angle, and θ_k is the roll angle. In the case of wheelsets, the following terminology is used for the corresponding angles: ψ_i is called "angle of attack", φ_i is called "wheelset rotation angle", and $d\varphi_i/dt$ is the angular velocity of the i^{th} wheelset around axis y_i.

Individual bodies in the railway vehicle model are connected with each other by flexible (spring-damping) links, which constitute the vehicle suspension system. In most railway vehicles, including passenger carriages, two-stage suspension systems are used: the primary suspension (springing) system consists of the flexible links between wheelsets and bogie frames and the secondary suspension (springing) system consists of the flexible links between the bogie frames and the vehicle body. In conventional railway cars with passive suspension systems, the typical suspension components include coil springs and hydraulic dampers. In the railway vehicle model presented, the suspension components are treated as zero-mass elements and their force-deflection curves are approximated by linear functions of suspension element deformations and of time derivatives of the deformations. Such characteristic curves correspond to those of the rheological models consisting of a spring with stiffness coefficient k and a viscous damper with damping coefficient c.

In this study, the original model of a railway vehicle (Figs. 1a and 1b) is simplified at first to a half-vehicle model shown in Figs. 1c and 1d. In order to determine the mass m_{bp} of the vehicle body part taken into account in the simplified model, the vehicle body is represented by a system of three point masses m_{bp}, m_{bs}, and m_{bt}, situated in the central axis of inertia of the vehicle body (directed along axis Ox), i.e. in the centre of vehicle body mass and at points situated at distances of $l_p = l_t = l_w/2$ from the said centre to the front and rear of the vehicle

body, respectively (Fig. 1e). The vehicle body mass has been divided into masses m_{bp}, m_{bs}, and m_{bt} in compliance with three rules: mass conservation law (the first equation in Fig. 1e), law of conservation of the position of the centre of mass (the second equation in Fig. 1e), and law of conservation of the moment of inertia with respect to axis Oy (the third equation in Fig. 1e). Such a method of determining the equivalent mass of the vehicle body in the half-vehicle model is more accurate from the point of view of vehicle dynamics than the adopting of $m_{bp} = m_b/4$, as it was done for the quarter-vehicle model in the work described in Liang et al. (2012).

At the next stage, the model is further reduced so that it becomes applicable to the description of motion of the vehicle model bodies in the vertical direction only. Thus, a reduced half-vehicle model (Fig. 2) is built, which is a system with two degrees of freedom (a 2DOF system) describing the vertical vibrations of a part of the vehicle body ("sprung mass") situated over one of the bogies and vibrations of the masses connected with the bogie frame ("unsprung mass"). The two mass elements are connected with each other by a spring-damper system acting in parallel and representing the spring-damping properties of the secondary suspension system, elsewhere referred to (for simplification) as "suspension system". The unsprung mass interacts with the equivalent rail wheel (representing two wheelsets of the bogie under consideration) through a spring-damper or spring-only element, which represents the spring-damping or spring-only properties of the primary suspension system.

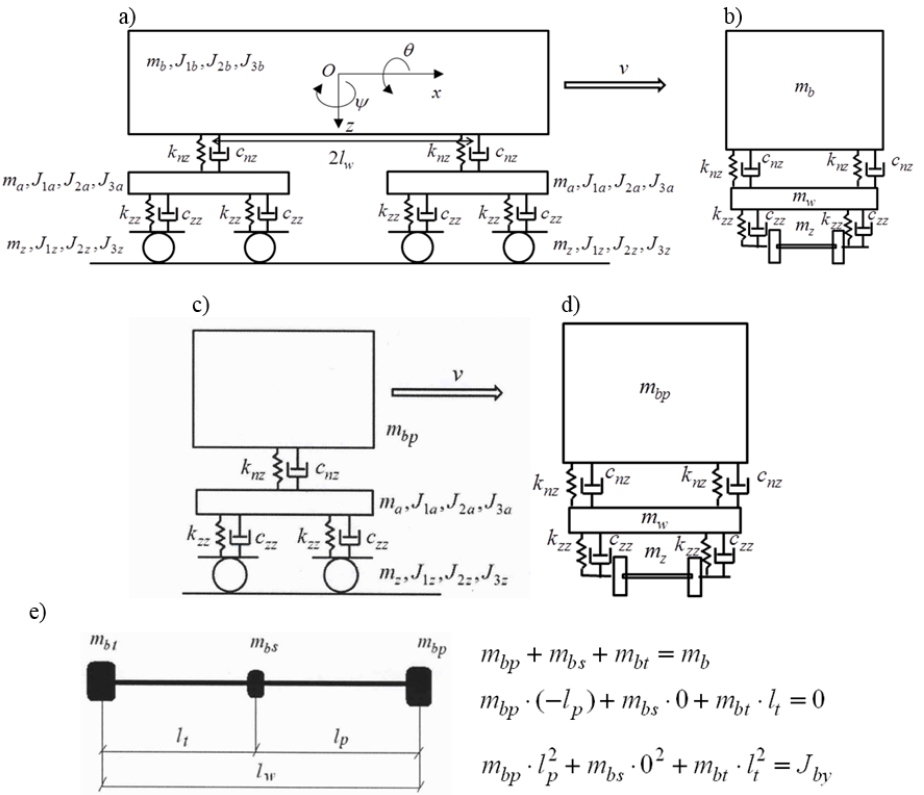

Fig. 1. Original physical model of a passenger carriage, viewed in plane (*x*, *z*) (Fig. a) and in plane (*y*, *z*) (Fig. b), and simplified half-vehicle model of the carriage, viewed in plane (*x*, *z*) (Fig. c) and in plane (*y*, *z*) (Fig. d); illustration of the method of determining masses m_{bp} and m_{bt} of vehicle body halves and coupling mass m_{bs} (Fig. e)

The parameters of this reduced model have been determined on the grounds of the half-vehicle model shown in Fig. 1. In particular, the sprung mass is $m_1 = m_{bp}$, the unsprung mass m_2 is equal to the bogie frame mass m_w, and the equivalent rail wheel mass m_z has been adopted as the total mass of two wheelsets. The stiffness and damping coefficients of the primary suspension system, denoted by k_2 and c_2, respectively, have been determined as sums of appropriate coefficients k_{zz} and c_{zz} of the four spring-damping links that are components of the primary vertical suspension system and are situated on the left and right side of each of the two wheelsets included in the bogie. In consequence, the coefficient values are $k_2 = 4k_{zz}$ and $c_2 = 4c_{zz}$. The stiffness and damping coefficients of the secondary suspension system $k_1 = 2k_{nz}$ and $c_1 = 2c_{nz}$ have been determined likewise, by adding up the values of the corresponding coefficients of the two components of the secondary vertical suspension system, situated on the left and right side of the bogie.

3. Objective

The objective of this study is to present the methods of optimizing the characteristics of a passive secondary suspension system of a railway car, elsewhere referred to (for simplification) as "suspension system". A linear half-vehicle model and an example procedure of determining the suspension damping coefficient has been used.

In this study, over 40-year achievements of the cited authors of publications in the field of motor vehicle dynamics have been utilized as an alternative for the methodology normally used in the railway engineering for the selection of damping in the suspension system of a railway vehicle. The work also contributes to the development of the standard methods.

Previously, the impact of parameters of the passive suspension system on the dynamics of a railway vehicle, especially on the ride comfort, was examined and the results have been given in publications (Kardas-Cinal, 2013, Kardas-Cinal, 2006; Kisilowski, 1991; Zhou et al., 2009). As regards active vehicle suspension systems, the research works on such systems have been presented e.g. in (Kim et al., 2007; Li & Goodall, 1999; Liang et al., 2012; Orvnäs, 2010; Orvnäs, 2011; Sim et al., 2013).

The algorithms adopted for the calculations have a wider range of applicability; especially, they may be used for determining the optimum values of the other parameters of the railway vehicle model under analysis, i.e. stiffness of the secondary suspension system as well as stiffness and damping of the primary suspension system.

4. Detailed description of the half-vehicle model and its equations of motion in the time and frequency domain

Below has been given a detailed description of the linear half-vehicle model presented in Fig. 2. It consists of three mass elements, i.e. sprung mass m_1 [kg] (a part of the vehicle body), unsprung mass m_2 [kg] (connected with the bogie frame), and equivalent rail wheel mass m_z [kg] representing the mass of two wheelsets of the specific railway car bogie. The stiffness coefficients of the secondary suspension system, elsewhere referred to (for simplification) as "suspension system", and of the primary suspension system have been denoted by k_1 [N/m] and k_2 [N/m], respectively. The symbols c_1 [N·s/m] and c_2 [N·s/m] have the meaning of the viscous damping coefficients of the secondary and primary suspension systems, respectively. The quantity denoted by ζ (t) [m] is the time-varying vertical kinematic excitation caused by track profile irregularities. The rail wheel (wheelsets) lift-off phenomenon is disregarded. The railway vehicle, i.e. the model under consideration as well, moves rectilinearly with a constant speed V [km/h] (i.e. v [m/s]).

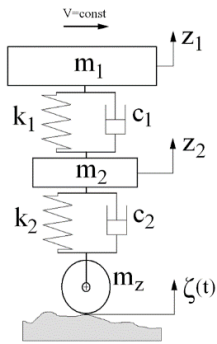

Fig. 2. Half-vehicle model (for the notation used, see the text)

The equations of motion may be derived from the kinetostatic analysis, with taking into account the forces of inertia of the mass elements of the model. They have the form as presented in relation (1).

$$\begin{cases} m_1 \cdot \ddot{z}_1 + c_1 \cdot \dot{z}_1 + k_1 \cdot z_1 - c_1 \cdot \dot{z}_2 - k_1 \cdot z_2 = 0 \\ m_2 \cdot \ddot{z}_2 + (c_1 + c_2) \cdot \dot{z}_2 + (k_1 + k_2) \cdot z_2 - c_1 \cdot \dot{z}_1 - k_1 \cdot z_1 = c_2 \cdot \dot{\zeta} + k_2 \cdot \zeta \end{cases} \quad (1)$$

$$\underbrace{\begin{bmatrix} m_1 & 0 \\ 0 & m_2 \end{bmatrix}}_{\mathbf{M}} \cdot \underbrace{\begin{bmatrix} \ddot{z}_1 \\ \ddot{z}_2 \end{bmatrix}}_{\ddot{\mathbf{q}}} + \underbrace{\begin{bmatrix} c_1 & -c_1 \\ -c_1 & c_1 + c_2 \end{bmatrix}}_{\mathbf{C}} \cdot \underbrace{\begin{bmatrix} \dot{z}_1 \\ \dot{z}_2 \end{bmatrix}}_{\dot{\mathbf{q}}} + \underbrace{\begin{bmatrix} k_1 & -k_1 \\ -k_1 & k_1 + k_2 \end{bmatrix}}_{\mathbf{K}} \cdot \underbrace{\begin{bmatrix} z_1 \\ z_2 \end{bmatrix}}_{\mathbf{q}} = \underbrace{\begin{bmatrix} 0 \\ c_2 \end{bmatrix}}_{\mathbf{C}_\zeta} \cdot \dot{\zeta} + \underbrace{\begin{bmatrix} 0 \\ k_2 \end{bmatrix}}_{\mathbf{K}_\zeta} \cdot \zeta \quad (2)$$

Their matrix form is shown in relation (2), where the symbols of the matrices of inertia **M**, viscous damping **C**, stiffness **K**, excitation influences transmitted by the viscous damping in the primary suspension system $\mathbf{C}_\zeta$, and excitation influences transmitted by the stiffness of the primary suspension system $\mathbf{K}_\zeta$ have been indicated. The vectors of the generalized coordinates (displacements), velocities, and accelerations have been denoted by $\mathbf{q}, \dot{\mathbf{q}}, \ddot{\mathbf{q}}$, respectively. This notation has been adopted in relation (equation) (3), which is the most concise form of presenting the relation (1).

$$\mathbf{M} \cdot \ddot{\mathbf{q}} + \mathbf{C} \cdot \dot{\mathbf{q}} + \mathbf{K} \cdot \mathbf{q} = \mathbf{C}_\zeta \cdot \dot{\zeta} + \mathbf{K}_\zeta \cdot \zeta \quad (3)$$

For equation (3), the Laplace transform has been formulated, for zero initial conditions. After transformations, equation (4) has been obtained, where the domain $s = r + i \cdot \omega$ has a real part r and an imaginary part ω, while $i^2 = -1$ (ω is the angular frequency [rad/s]):

$$\left(\mathbf{M} \cdot s^2 + \mathbf{C} \cdot s + \mathbf{K}\right) \cdot \mathbf{q}(s) = \left(\mathbf{C}_\zeta \cdot s + \mathbf{K}_\zeta\right) \cdot \zeta(s) \quad (4)$$

The solution of this equation has the form (5):

$$\mathbf{q}(s) = \left(\mathbf{M} \cdot \mathbf{s}^2 + \mathbf{C} \cdot \mathbf{s} + \mathbf{K}\right)^{-1} \cdot \left(\mathbf{C}_\zeta \cdot \mathbf{s} + \mathbf{K}_\zeta\right) \cdot \zeta(s) \quad (5)$$

The operational transmittance (transfer function) for displacements (6) is the ratio of the Laplace transform of the output signal (response) of a system to the Laplace transform of the input signal (excitation) of the same system at zero initial conditions:

$$\mathbf{H}_\mathbf{q}(\mathbf{s}) = \begin{bmatrix} H_{q_1}(s) \\ H_{q_2}(s) \end{bmatrix} = \frac{\mathbf{q(s)}}{\zeta(s)} = \left(\mathbf{M} \cdot \mathbf{s}^2 + \mathbf{C} \cdot \mathbf{s} + \mathbf{K}\right)^{-1} \cdot \left(\mathbf{C}_\zeta \cdot \mathbf{s} + \mathbf{K}_\zeta\right) \quad (6)$$

The operational transmittances for velocities and accelerations are expressed by relations (7) and (8), respectively:

$$\mathbf{H}_{\dot{\mathbf{q}}}(\mathbf{s}) = \begin{bmatrix} H_{\dot{q}_1}(s) \\ H_{\dot{q}_2}(s) \end{bmatrix} = \frac{\dot{\mathbf{q}}(\mathbf{s})}{\zeta(s)} = \mathbf{s} \cdot \mathbf{H}_\mathbf{q}(\mathbf{s}) \quad (7)$$

$$\mathbf{H}_{\ddot{\mathbf{q}}}(\mathbf{s}) = \begin{bmatrix} H_{\ddot{q}_1}(s) \\ H_{\ddot{q}_2}(s) \end{bmatrix} = \frac{\ddot{\mathbf{q}}(\mathbf{s})}{\zeta(s)} = \mathbf{s}^2 \cdot \mathbf{H}_\mathbf{q}(\mathbf{s}) \quad (8)$$

We can easily pass from the Laplace transform to the Fourier transform. The operational transmittances will then become spectral transmittances. In formal terms, this is expressed in passing from domain s to argument $i \cdot \omega$, by assuming the real part r of the expression $s = r + i \cdot \omega$ as zero. With such a substitution, the relations (4)-(8) still hold.

5. Random excitation from track profile irregularities

An assumption has been made here that the track is undeformable but uneven in the vertical direction. The track profile irregularities constitute a realization of a stationary Gaussian random process. The track of a specific class is described in ORE B176 (1989) by the function of power spectral density (PSD) $S_d(\Omega)$ [m³/rad] of the vertical profile irregularities:

$$S_d(\Omega) = \frac{A \cdot \Omega_c^2}{(\Omega^2 + \Omega_c^2) \cdot (\Omega^2 + \Omega_r^2)} \quad (9)$$

where:
- $\Omega = 2\pi/L = 2\pi \cdot f_s$ – angular (spatial) frequency of the track profile [rad/m];
- L – wavelength of track profile irregularities [m];
- f_s – track profile wave number (spatial frequency) [1/m];
- Ω_c = 0.8200 rad/m;
- Ω_r = 0.0206 rad/m;

A = 4.032e-07 m^2·rad/m for a "good-quality" ("low-disturbance") track;
A = 10.800e-07 m^2·rad/m for a "poor-quality" ("high-disturbance") track.

The presented form of the PSD function $S_d(\Omega)$ of the vertical profile irregularities is defined for the angular (spatial) frequency Ω of the track profile being within the interval $0.0628 \text{ rad/m} \le \Omega \le 2.513 \text{ rad/m}$, i.e. for the wave number (spatial frequency) f_s being within the interval $0.01 \text{ 1/m} \le f_s \le 0.4 \text{ 1/m}$, which corresponds to the wavelength L ranging from 2.5 m to 100 m. For the f_s values exceeding the upper limit, the S_d values have been assumed as zero. The PSD values of the vertical profile irregularities for a "good-quality" and "poor-quality" track, according to the classification given in ORE B176 (1989), have been shown in Fig. 3.

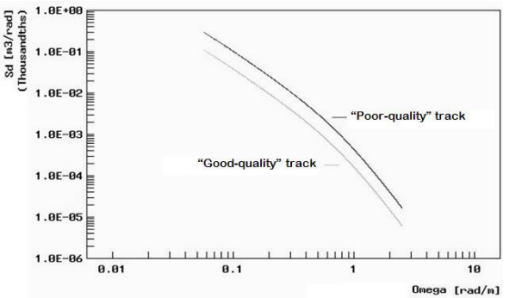

Fig. 3. Power spectral density values of random track profile irregularities according to the classification given in ORE B176 (1989)

6. Criteria of the selection of damping in the half-vehicle suspension system (optimization criteria)

In the half-vehicle model, only the vertical motion is analysed. As it was in publications (Crolla, 1996; Firth, 1991; Gobbi et al., 2006; Gobbi & Mastinu, 2001; Kasprzyk & Prochowski, 1990, Kasprzyk et al., 1974; Mitschke, 1989; Mitschke, 1977; Muluka, 1998; Orvnäs, 2010; Orvnäs, 2011; Otenberg, 1974; Ryba, 1974; Sekulić & Devidović, 2011; Sharp & Crolla, 1987; Sharp & Hassan, 1986; Ślaski, 2012; Verros et al., 2005; Wong, 2001), three criteria have been adopted to assess the correctness of selection of suspension damping coefficient c_1:

– minimization of vehicle occupants' discomfort, which is measured by the standard deviation of sprung mass acceleration, σ_a [m/s^2];
– minimization of the safety hazard, which is measured by the standard deviation of the varying dynamic component (i.e. the dynamic value measured in relation to the static value) of the vertical reaction at the wheel-rail contact, σ_F [N];
– reduction in the working displacements of the secondary suspension system to a value lower than the secondary suspension displacement limit r_{zg} [m].

In formal terms, these criteria may be described as follows (as functions of suspension damping coefficient c_1 and vehicle speed V):

$$Q(c_1, V) = w_a \cdot \sigma_a(c_1,V) + w_F \cdot \sigma_F(c_1,V) \Rightarrow \min \quad (10)$$

$$6 \cdot \sigma_{uz}(c_1, V) \le r_{zg} \quad (11)$$

where:

$Q(c_1, V)$ [-] – the objective function subject to minimization;
w_a [1/m], w_F [1/N] – weighting factors for discomfort and safety hazard, respectively;
$\sigma_{uz}(c_1, V)$ [m] – standard deviation of the deflection of the secondary suspension system (measured in relation to the static value);
r_{zg} [m] – secondary suspension displacement limit.

The above criteria are adopted for each of all the track irregularity classes taken into consideration. The factor "6" in formula (11) comes from the Gaussian distribution of the suspension deflection in the model under analysis. This stems from the known property of the response of a linear system to a Gaussian stationary excitation from track profile irregularities, as these irregularities have Gaussian distributions, too. The working displacement of the secondary suspension system is treated here as a doubled value of the maximum dynamic deflection of the suspension system, which is equal to about $3 \cdot \sigma_{uz}$. The standard deviations σ_a, σ_F, and σ_{uz} are calculated from the following known formulas (Arczyński, 1993; Kamiński & Pokorski, 1983; Lozia, 2016; Mitschke, 1989; Mitschke, 1977; Osiecki, 1994; Otenberg, 1974; Wong, 2001):

$$\sigma_a = \sqrt{\int_0^{\omega_{max}} S_{\ddot{q}_1}(\omega) \cdot d\omega} = \sqrt{\int_0^{\omega_{max}} \left|H_{\ddot{q}_1}(i \cdot \omega)\right|^2 \cdot S_d(\omega) \cdot d\omega} \quad (12)$$

$$\sigma_F = \sqrt{\int_0^{\omega_{max}} S_F(\omega) \cdot d\omega} = \sqrt{\int_0^{\omega_{max}} \left|H_F(i \cdot \omega)\right|^2 \cdot S_d(\omega) \cdot d\omega} \quad (13)$$

$$\sigma_{uz} = \sqrt{\int_0^{\omega_{max}} S_{uz}(\omega) \cdot d\omega} = \sqrt{\int_0^{\omega_{max}} \left|H_{uz}(i \cdot \omega)\right|^2 \cdot S_d(\omega) \cdot d\omega} \quad (14)$$

where the new symbols are defined as follows:

$S_{\ddot{q}_1}(\omega), S_F(\omega), S_{uz}(\omega)$ – power spectral densities of sprung mass accelerations [m^2/s^3/rad], dynamic component of the vertical reaction at the wheel-rail contact [N^2·s/rad], and deflection of the secondary suspension system [m^2·s/rad], respectively;

$\omega = 2\pi \cdot f$ – radian frequency ω [rad/s] and Hertz frequency f [Hz];

$\omega_{max} = 2\pi \cdot f_{max}$ – maximum radian frequency ω_{max} [rad/s] and maximum Hertz frequency f_{max} [Hz] under consideration;

$H_{\ddot{q}_1}(i \cdot \omega)$ – spectral transmittance for the sprung mass acceleration (see 8) [$1/s^2$];

H_F (i·ω) – spectral transmittance for the dynamic component of the vertical reaction at the wheel-rail contact [N/m];

H_{uz} (i·ω) – spectral transmittance for the deflection of the secondary suspension system [-].

To pass from $S_d(\Omega)$ [m^3/rad] to $S_d(\omega)$ [m^2·s/rad], i.e. to change the independent variable from Ω [rad/m] (angular, i.e. spatial, frequency of the track profile) to ω [rad/s] (radian frequency of the input vibration), Ω must be multiplied by vehicle speed v [m/s], with $S_d(\Omega)$ being simultaneously divided by v [m/s]. Thanks to this, the definite integrals of $S_d(\Omega)$ and $S_d(\omega)$ in the mutually corresponding frequency bands under consideration (Ω and ω) will have the same value: the variance of track profile height (σ_ξ^2).

The Fourier transforms of the dynamic component of the vertical reaction at the wheel-rail contact and of the deflection of the secondary suspension system are defined by the following two equations, respectively:

$$F(i \cdot \omega) = c_2 \cdot [\dot{\xi}(i \cdot \omega) - \dot{z}_2(i \cdot \omega)] + k_2 \cdot [\xi(i \cdot \omega) - z_2(i \cdot \omega)] + m_z \cdot \ddot{\zeta}(i \cdot \omega) \quad (15)$$

$$u_z(i \cdot \omega) = z_2(i \cdot \omega) - z_1(i \cdot \omega) \quad (16)$$

Based on equations (6)-(8) as well as (15) and (16), after transformations, the following final concise forms of spectral transmittances have been obtained (with remembering that $q_1 = z_1$ and $q_2 = z_2$):

$$H_{\ddot{q}_1}(i \cdot \omega) = \frac{\ddot{q}_1(i \cdot \omega)}{\zeta(i \cdot \omega)} = -\omega^2 \cdot H_{q_1}(i \cdot \omega) \quad (17)$$

$$H_F(i \cdot \omega) = \frac{F(i \cdot \omega)}{\zeta(i \cdot \omega)} = (i \cdot c_2 \cdot \omega + k_2) \cdot [1 - H_{q_2}(i \cdot \omega)] - m_z \cdot \omega^2 \quad (18)$$

$$H_{uz}(i \cdot \omega) = \frac{q_2(i \cdot \omega) - q_1(i \cdot \omega)}{\zeta(i \cdot \omega)} = H_{q_2}(i \cdot \omega) - H_{q_1}(i \cdot \omega) \quad (19)$$

7. Calculation data: parameters of the model and of the test conditions

The model parameters taken as an example, corresponding to the data of the suspension system of a passenger carriage, have been given in Table 1. Two tracks, described in Section 5, were chosen for the calculations:

– track 1, referred to as a "good-quality" (or "low-disturbance") track;
– track 2, referred to as a "poor-quality" (or "high-disturbance") track.

The lowest and highest values of the wavelength of track profile irregularities were L = 2.5 m and L = 100 m, respectively. For the frequencies exceeding the upper limit of this frequency band, the PSD values $S_d(\Omega)$ of the vertical track profile irregularities have been assumed as zero.

In consideration of the ISO standard provisions that concern the vibrational comfort (ISO 2631–1, 1985 & 1997), the frequency band of 0-80 Hz (0-502.65 rad/s) was adopted for the analyses.

The analyses were carried out for 12 constant vehicle speeds V [km/h], changed within the range from 50 km/h to 160 km/h in steps of 10 km/h. The vehicle speed values expressed as v [m/s] and V [km/h] are connected with each other by the generally known relation v = V/3.6.

The damping coefficient c_1 [N·s/m] was changed and its values were indirectly expressed by means of a relative damping coefficient (Arczyński, 1993) for the secondary suspension system, i.e. by values γ [-] defined as follows:

$$\gamma = \frac{c_1}{c_{1kr}} = \frac{c_1}{2 \cdot m_1 \cdot \omega_{01}} = \frac{h}{\omega_{01}} \quad (20)$$

$$c_{1kr} = 2 \cdot m_1 \cdot \omega_{01} \quad (21)$$

$$h = c_1/2/m_1 \quad (22)$$

where:

c_{1kr} [N·s/m] – critical damping coefficient for the secondary suspension system;

$\omega_{01} = 2\cdot\pi\cdot f_{01}$ – the first (lower) natural radian frequency of the undamped system [rad/s];

f_{01} – the first (lower) natural Hertz frequency of the undamped system [Hz];

$$\omega_{01}^2 = \frac{k_1\cdot m_2 + (k_1+k_2)\cdot m_1}{2\cdot m_1\cdot m_2} - \sqrt{\left[\frac{k_1\cdot m_2 + (k_1+k_2)\cdot m_1}{2\cdot m_1\cdot m_2}\right]^2 - \frac{k_1\cdot k_{21}}{m_1\cdot m_2}} \quad (23)$$

The second (higher) natural radian frequency of the undamped system $\omega_{02} = 2\cdot\pi\cdot f_{02}$ [rad/s] is defined by the following equation (Arczyński, 1993):

$$\omega_{02}^2 = \frac{k_1\cdot m_2 + (k_1+k_2)\cdot m_1}{2\cdot m_1\cdot m_2} + \sqrt{\left[\frac{k_1\cdot m_2 + (k_1+k_2)\cdot m_1}{2\cdot m_1\cdot m_2}\right]^2 - \frac{k_1\cdot k_{21}}{m_1\cdot m_2}} \quad (24)$$

and f_{02} is the second (higher) natural Hertz frequency of the undamped system [Hz].

For the system under analysis, these values were ω_{01} = 8.715 rad/s, ω_{02} = 31.567 rad/s, f_{01} = 1.387 Hz, f_{02} = 5.024 Hz, c_{1kr} = 123 969.258 N·s/m ≈ 123 970 N·s/m.

The analyses were carried out for 26 values of the relative damping coefficient γ [-], changed within the range from 0.2 to 0.7 in steps of 0.02.

The value of the coefficient of damping in the suspension system was:

$$c_1 = \gamma\cdot c_{1kr} = \gamma\cdot 2\cdot m_1\cdot\omega_{01}\ [\mathrm{N\cdot s/m}] \quad (25)$$

The weighting factors for discomfort and safety hazard, w_a and w_F, were so selected that they reflected equal treatment of both of these criteria. In the easiest way, their values should be determined after the stage of normalization of calculation results, which has been described in Lozia (2016).

The working displacements of the suspension system were limited to a value of r_{zg} = 0.0985 m, corresponding to the real linear range of operation of the suspension system of the railway vehicle under analysis. The model parameters and test conditions as described above have been brought together in Table 1.

8. Calculation results before the modification of the optimization criteria

For the model parameters and test conditions as specified in Table 1, calculations were carried out in accordance with the algorithm presented in a previous part of this paper.

Figs. 4, 5, and 6 show the absolute values of spectral transmittances for sprung mass acceleration, for the dynamic component of the vertical reaction at the wheel-rail contact, and for the deflection of the secondary suspension system, as functions of the excitation frequency, in the 0-80 Hz frequency band, for various values of the relative damping coefficient, ranging from 0.2 to 0.7. In each of the three drawings mentioned above, a maximum can be clearly seen for a frequency close to the first natural frequency of the undamped system (1.387 Hz), with the values of the maximum being the lower the higher the relative damping was. The second resonance effect cannot be seen because of a high value of the coefficient of damping in the primary suspension system (c_2). For this hypothesis to be verified, calculations were also carried out for a significantly lower value of this damping coefficient. For such a case, the effect of the second natural frequency of the undamped system (5.024 Hz) could be clearly seen in graphs similar to those presented in Figs. 4, 5, and 6.

For the sprung mass acceleration (Fig. 4), the impact of damping was very high in the whole excitation frequency band under analysis. Apart from a drop in the absolute transmittance value with an increase in the damping in the zone close to the first resonance, a significant growth in the absolute transmittance value could be observed in the above-resonance zone. In the latter case, a growth in the damping impairs the ride comfort.

As regards the dynamic component of the vertical reaction at the wheel-rail contact (Fig. 5), the influence of damping was considerable at the excitation frequencies being low and close to the resonance (Fig. 5b). An increase in the damping reduced the absolute transmittance value in the area close to the first resonance and caused it to grow in the zone above the node in the graph curves, at frequencies exceeding 2 Hz. On the other hand, this impact was not so strong at the frequencies significantly exceeding the second resonance, where the absolute transmittance values remained close to

each other in spite of increasing frequencies (Fig. 5a).
The absolute value of the spectral transmittance of suspension deflection (Fig. 6) declined with increasing damping in the area close to the first resonance. In the above-resonance zone, this impact of the damping in the suspension system was quite small.

Table 1. List of the model parameters and test conditions

Item	Description	Symbol	Unit	Value
1.	Mass of the part of the vehicle body solid, "sprung mass"	m_1	kg	7 112
2.	Mass connected with the bogie frame, "unsprung mass"	m_2	kg	2 707
3.	Mass of the equivalent rail wheel	m_z	kg	2 750
4.	Suspension stiffness	k_1	N/m	828 000
5.	Stiffness of the primary suspension system	k_2	N/m	1 760 000
6.	Damping coefficient of the secondary suspension system	c_1	N·s/m	variable
7.	Damping coefficient of the primary suspension system	c_2	N·s/m	340 000
8.	Type and power spectral density parameters of the first test track	Track 1: "good quality"	–	–
9.	Constant value that occurs in the formula (9)	Ω_c	rad/m	0.8200
10.	Constant value that occurs in the formula (9)	Ω_r	rad/m	0.0206
11.	Constant value that occurs in the formula (9)	A	m^2·rad/m	4.032e-07
12.	Type and power spectral density parameters of the second test track	Track 2: "poor quality"	–	–
13.	Constant value that occurs in the formula (9)	Ω_c	rad/m	0.8200
14.	Constant value that occurs in the formula (9)	Ω_r	rad/m	0.0206
15.	Constant value that occurs in the formula (9)	A	m^2·rad/m	10.800e-07
16.	Minimum wavelength of track profile irregularities	L_{min}	m	2.5
17.	Maximum wavelength of track profile irregularities	L_{max}	m	100.0
18.	Minimum Hertz (radian) frequency of the vibrations under analysis	f_{min} (ω_{min})	Hz (rad/s)	0 (0)
19.	Maximum Hertz (radian) frequency of the vibrations under analysis	f_{max} (ω_{max})	Hz (rad/s)	80 (502.65)
20.	The first natural Hertz (radian) frequency of the undamped system	f_{01} (ω_{01})	Hz (rad/s)	1.387 (8.715)
21.	The second natural Hertz (radian) frequency of the undamped system	f_{02} (ω_{02})	Hz (rad/s)	5.024 (31.567)
22.	Critical suspension damping coefficient	c_{1kr}	N·s/m	123 970
23.	Vehicle speed range under analysis	V_{min}-V_{max} (v_{min}-v_{max})	km/h (m/s)	50.0-160.0 (13.89-44.44)
24.	Vehicle speed sampling step	ΔV (Δv)	km/h (m/s)	10.0 (2.78)
25.	Minimum value of the relative suspension damping coefficient	γ_{min}	–	0.2
26.	Maximum value of the relative suspension damping coefficient	γ_{max}	–	0.7
27.	Sampling step of the relative suspension damping coefficient	$\Delta\gamma$	–	0.02
28.	Secondary suspension displacement limit	r_{zg}	m	0.0985

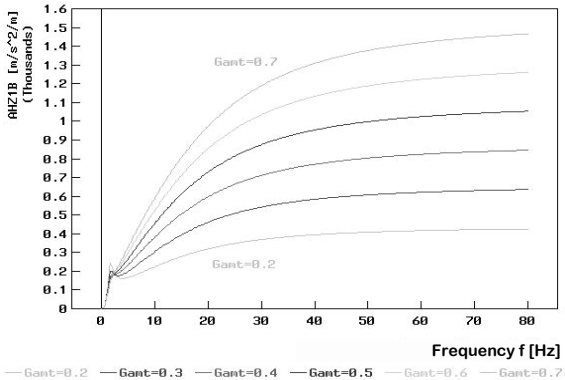

Fig. 4. Absolute value of the spectral transmittance for sprung mass acceleration (see formulas (8) and (19), denoted by AHZ1B in the graph) vs. excitation frequency f, for various values of the relative damping coefficient (see formula (22), denoted by Gamt in the graph)

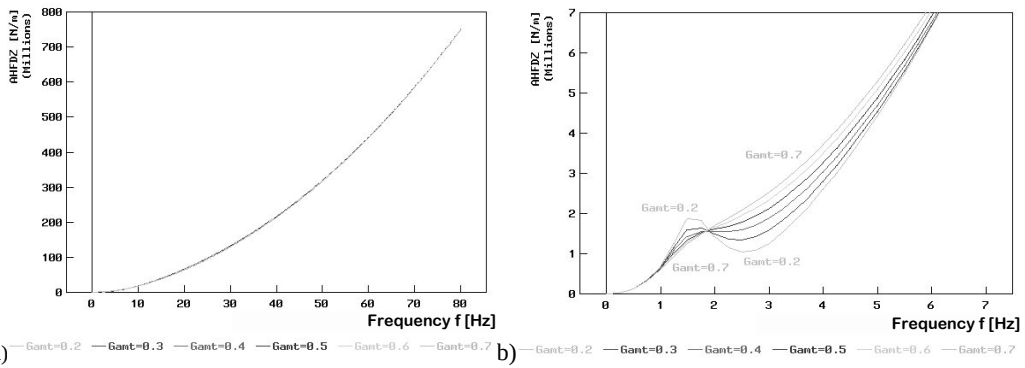

a) b)

Fig. 5. Absolute value of the spectral transmittance for the dynamic component of the vertical reaction at the wheel-rail contact (see formulas (17) and (20), denoted by AHFDZ in the graph) vs. excitation frequency f, for various values of the relative damping coefficient (see formula (22), denoted by Gamt in the graph): a) curve plotted for the whole range of variability of f and AHFDZ; b) magnified fragment of this curve for the frequency range 0-7 Hz

Examples of power spectral density of track profile irregularities $S_d(\omega)$ for the track classified in ORE B176 (1989) as a track of "poor quality" have been shown (in a log-log scale) in Fig. 7 as functions of the radian frequency ω [rad/s] for various vehicle speeds (V = 50-160 km/h). The independent variable has been presented (after appropriate conversion) as excitation frequency f [Hz], exclusively for presentation needs, i.e. for easier comparisons with other graphs included in this study. An increase in the vehicle speed translates into a growth in the excitation frequencies f [Hz] corresponding to the lower and upper limit of the track profile wavelength L (2.5 m and 100 m, respectively). The lower frequency limit, corresponding to the wavelength of 100 m, varies from 0.139 Hz for 50 km/h to 0.444 Hz for 160 km/h. Such changes are hardly noticeable in Fig. 7 due to the scale adopted. The changes in the upper frequency limit, corresponding to the wavelength of 2.5 m, can be easier noticed: the upper frequency limit changes from 5.556 Hz for 50 km/h to 17.778 Hz for 160 km/h. A drop in the $S_d(\omega)$ for the upper frequency limit, corresponding to the shortest wavelength L = 2.5 m, can be seen as well. This is caused by the dividing of $S_d(\Omega)$ by vehicle speed v in order to obtain the $S_d(\omega)$ value, as mentioned in Section 6.

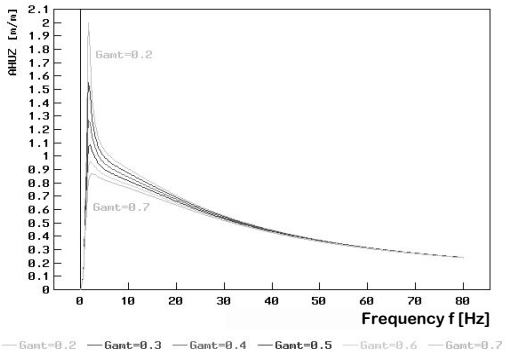

Fig. 6. Absolute value of the spectral transmittance for the deflection of the secondary suspension system (see formulas (18) and (21), denoted by AHUZ in the graph) vs. excitation frequency f, for various values of the relative damping coefficient (see formula (22), denoted by Gamt in the graph)

Figs. 8, 9, and 10 show (in a log-log scale) power spectral densities as functions of excitation frequency f for the quantities that were taken as a basis for calculations of the criteria of assessment of the system under analysis. The graphs have been plotted for the track classified as "poor" according to ORE B176 (1989) and for a vehicle speed of V = 110 km/h. The curves differ from each other in the values of the relative suspension damping coefficient (see formula (20)). Fig. 8 shows the power spectral densities of sprung mass accelerations (see the element of integration in equation (12)), Fig. 9 shows the power spectral densities of the dynamic component of the vertical reaction at the wheel-rail contact (see the element of integration in equation (13)), and Fig. 10 shows the power spectral densities of the deflection of the secondary suspension system (see the element of integration in equation (14)). The analogical results obtained for the track classified as "good" according to ORE B176 (1989) are similar in qualitative terms; they differ from those related to the "poor" track in the values of the results obtained, which are lower in this case.

In all the three drawings mentioned above, a distinct impact of the relative damping and of the resonance frequencies of the undamped system (1.387 Hz and 5.024 Hz, especially the former one, as mentioned previously) on the shape of the curves plotted can be seen. For the sprung mass accelerations (Fig. 8), the impact of the damping was high for the first resonance (the damping reduced the power spectral density values) and in the zone above 2 Hz (where a growth in the damping caused the power spectral density to rise, and to a significant extent at that). For the dynamic component of the vertical reaction at the wheel-rail contact (Fig. 9), a growth in the damping reduced the power spectral density values in the first resonance zone and raised these values in the frequency range between 2 Hz and 8 Hz. This impact, however, was not very big at the frequencies exceeding 8 Hz. The values of the power spectral density of suspension deflection (Fig. 10) strongly depended on the suspension damping in the first resonance zone, where the dumping reduced the power spectral density values.

Standard deviations of the quantities taken as criteria of assessment of the system under analysis have been presented in Figs. 11, 12, and 13 as functions of the relative damping coefficient (see formula (20)), for the track classified as "poor" according to ORE B176 (1989) and for 12 vehicle speed values ranging from 50 km/h to 160 km/h. In Figs. 11 and 12, the minimums of the curves presented have been marked.

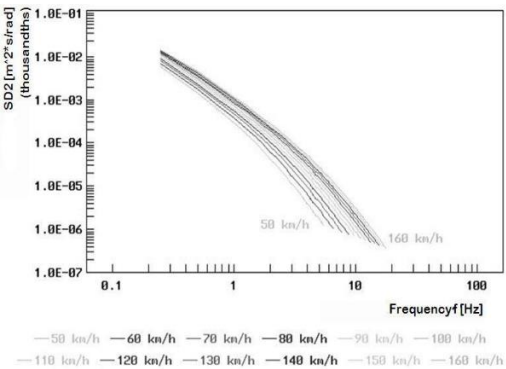

Fig. 7. Power spectral densities of track profile irregularities $S_d(\omega)$ (denoted by SD2 in the graph) vs. the radian frequency ω [rad/s], presented as Hertz frequency f [Hz] of the excitation (for easier comparisons with other graphs), for the track classified as "poor" according to ORE B176 (1989) and for various vehicle speeds V [km/h]

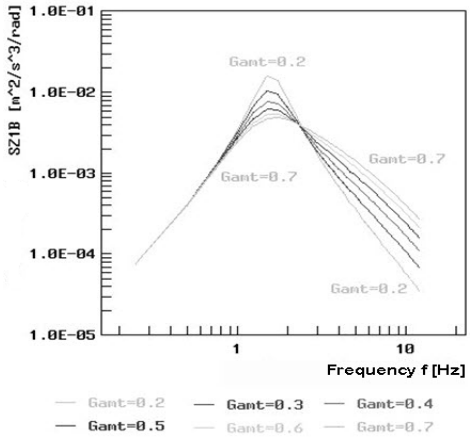

Fig. 8. Power spectral densities of sprung mass accelerations (denoted by SZ1B in the graph, see the element of integration in equation (12)) vs. excitation frequency f, for various values of the relative damping coefficient (see formula (20), denoted by Gamt in the graph), for the track classified as "poor" according ORE B176 (1989) and for a vehicle speed of V = 110 km/h

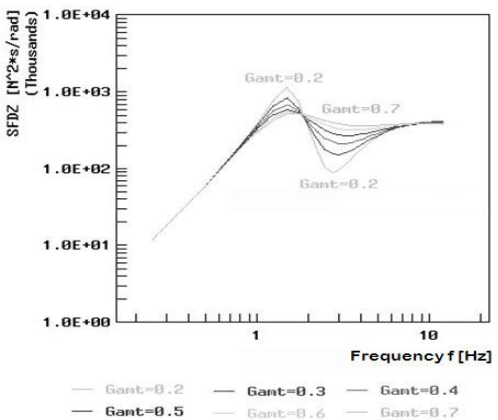

Fig. 9. Power spectral densities of the dynamic component of the vertical reaction at the wheel-rail contact (denoted by SFDZ in the graph, see the element of integration in equation (13)) vs. excitation frequency f, for various values of the relative damping coefficient (see formulas (20), denoted by Gamt in the graph), for the track classified as "poor" according to ORE B176 (1989) and for a vehicle speed of V = 110 km/h

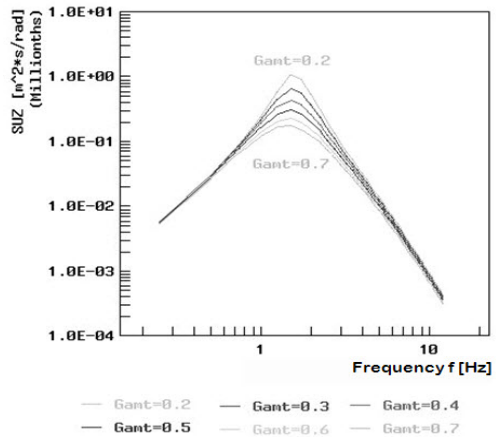

Fig. 10. Power spectral densities of suspension deflection (denoted by SUZ in the graph, see the element of integration in equation (14)) vs. excitation frequency f, for various values of the relative damping coefficient (see formulas (20), denoted by Gamt in the graph), for the track classified as "poor" according to ORE B176 (1989) and for a vehicle speed of V = 110 km/h

Fig. 11 shows the standard deviations of sprung mass accelerations (see formula (12)), Fig. 12 shows the standard deviations of the dynamic component of the vertical reaction at the wheel-rail contact (see formula (13)), and Fig. 13 shows the standard deviations of the deflection of the secondary suspension system (see formula (14)). The analogical results obtained for the track classified as "good" according to ORE B176 (1989) are similar in qualitative terms; they differ from each other in the values of the results obtained (for the "good" track, these values are lower), but the locations of the minimums are identical.

Fig. 13 clearly shows the existence of a monotonic trend towards lower values of the deflection of the secondary suspension system with increasing relative damping in this system. The intensity of this decrease, however, declines with the growth in the damping.

Fig. 14 shows the relative damping coefficient values (see formula (20), denoted by Gamt in the graph) that correspond to minimums of the standard deviation of the deflection of the secondary suspension system (denoted by Sig Z1bis in the graph) and minimums of the standard deviation of

the dynamic component of the vertical reaction at the wheel-rail contact (denoted by Sig Fd in the graph) for the track classified as "poor" according to ORE B176 (1989) versus vehicle speed values, which ranged from 50 km/h to 160 km/h. The analogical graph plotted for the track classified as "good" according to ORE B176 (1989) has an identical form.

Among the optimization criteria (10) and (11) proposed in Section 6, the one related to reduction in the working displacements of the suspension system (see formulas (11) and (14)) can be most easily applied and fulfilled. This is illustrated in Figs. 13a and 13b. The results considered as important are those obtained for the "poor quality" track (Fig. 13b). The value r_{zg} = 0.0985 m (Table 1) divided by 6 (see equation (11) is 0.01642 m and is much higher (i.e. about 4.8 times as high) as the highest value of σ_{uz} (c_1, V), which is about 0.0034, as presented in Fig. 13b.

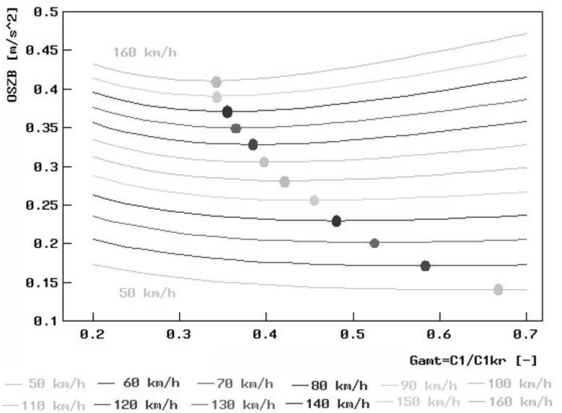

Fig. 11. Standard deviations of sprung mass accelerations (see (12), denoted by OSZB in the graph) vs. the relative damping coefficient (see formula (20), denoted by Gamt in the graph), for the track classified as "poor" according to ORE B176 (1989) and for 12 vehicle speed values ranging from 50 km/h to 160 km/h; the marks indicate the minimums of the curves presented

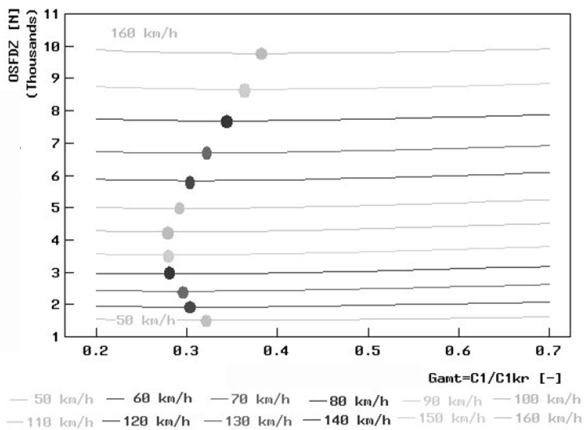

Fig. 12. Standard deviations of the dynamic component of the vertical reaction at the wheel-rail contact (see (13)), denoted by OSFDZ in the graph) vs. the relative damping coefficient (see formula (20), denoted by Gamt in the graph), for the track classified as "poor" according to ORE B176 (1989) and for 12 vehicle speed values ranging from 50 km/h to 160 km/h; the marks indicate the minimums of the curves presented

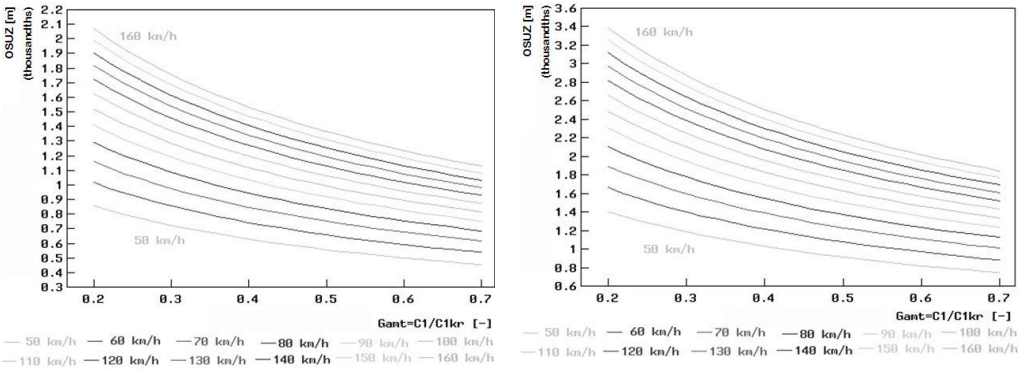

a) b)

Fig. 13. Standard deviations of the deflection of the secondary suspension system (see (14), denoted by OSUZ in the graphs) vs. the relative damping coefficient (see formula (20), denoted by Gamt in the graphs), for the tracks classified as "good" (Fig. a) and "poor" (Fig. b) according to ORE B176 (1989) and for 12 vehicle speed values ranging from 50 km/h to 160 km/h

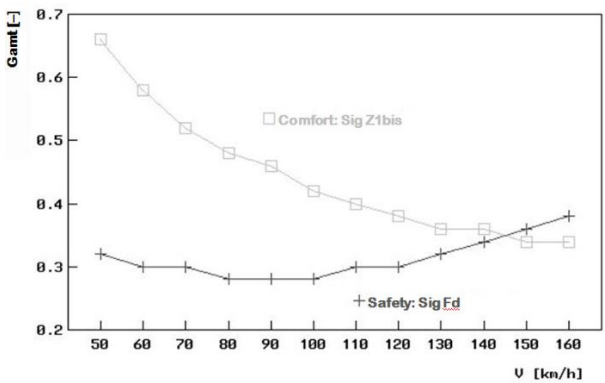

Fig. 14. Relative damping coefficient values (see formula (20), denoted by Gamt in the graph) that correspond to minimums of the standard deviation of the deflection of the secondary suspension system (denoted by Sig Z1bis in the graph) and minimums of the standard deviation of the dynamic component of the vertical reaction at the wheel-rail contact (denoted by Sig Fd in the graph) for the track classified as "poor" according to ORE B176 (1989) versus vehicle speed values, which ranged from 50 km/h to 160 km/h

The objective function Q (c_1) (see formula (10)) would create greater difficulties. Due to different measures of σ_a and σ_F, the weighting factors w_a and w_F cannot be dimensionless quantities. This problem was solved in the work described in [23] by normalization of functions σ_a (c_1, V) and σ_F (c_1, V). Another approach may also be tried, i.e. an attempt may be made to minimize the functions σ_a (c_1, V) and σ_F (c_1, V) separately.

The minimums of the standard deviations of sprung mass accelerations (Fig. 11) occurred for the relative damping coefficient values of a wide range from 0.34 to 0.66 and they largely depended on the vehicle speed, especially for the lower speed values. With growing vehicle speed, they were shifted towards the lower damping values. This is also well illustrated in Fig. 14. The strong dependence of the optimum value of the relative damping coefficient in the secondary suspension system on the vehicle speed as well as the presence of distinct minimums in the curves shown in Fig. 11 indicates the advisability of making the damping in this

suspension system dependent on the vehicle speed in accordance with the Sig Z1bis (V) curve in Fig. 14.

For the standard deviations of the dynamic component of the vertical reaction at the wheel-rail contact (Fig. 12), the minimums corresponded to the relative damping coefficient values ranging from 0.28 to 0.38. With growing vehicle speed, they showed a trend towards the lower values of the relative damping coefficient and, when the speed exceeded the level of 100 km/h, they began to move towards the higher values of the relative damping coefficient. The impact of the relative damping in the secondary suspension system on the standard deviations of the dynamic component of the vertical reaction at the wheel-rail contact, however, is insignificant: the curves describing its dependence on the vehicle speed (Fig. 12) are very flat. Hence, is seems to be fully justifiable to adopt the average value of the relative damping coefficient, equal to 0.33 (from the range of 0.28-0.38). The shapes of the curves presented in Figs. 11 and 12 (especially the flat shape of the curves in Fig. 12) provide grounds for giving priority to the criterion of the minimization of sprung mass acceleration.

9. Conclusion

In this study, over 40-year achievements of many foreign and Polish authors in the field of methods of optimizing the characteristics of passive suspension systems of vehicles have been summed up. Results of calculations carried out within work on the optimization of linear damping in the passive secondary suspension system of a railway vehicle moving on an uneven track with a random profile have been presented in detail. A half-vehicle model was used for this purpose.

The calculation results have been presented in the form of an objective function, which was adopted as a criterion of the optimization in respect of ride comfort and safety. The limitation of deflections of the suspension system has been taken into account, too.

The maximum suspension deflection values obtained and the described shapes of the curves that show the dependence of the criterial quantities on the vehicle speed and relative suspension damping coefficient provide grounds for giving priority to the criterion of the minimization of sprung mass acceleration. The presence of distinct minimums in the damping coefficient curves indicates the advisability of making the damping in the secondary suspension system dependent on the vehicle speed in accordance with the shape of the curve representing changes in this criterial function.

The algorithms adopted for the calculations have a wider range of applicability; especially, they may be used for determining the optimum values of the other model parameters, i.e. stiffness of the secondary suspension system as well as stiffness and damping of the primary suspension system.

The method presented is the first step in the process of optimizing the damping in the secondary suspension system of a railway vehicle. In further calculations, carried out with employing a half-vehicle model, such issues as nonlinearities of spring characteristics of the suspension system, asymmetry and nonlinearities of shock absorber characteristics, dry friction in the suspension system, and wheel lift-off should be taken into account.

The next step should include the use of three-dimensional vehicle motion models, which most accurately reflect the properties of a real vehicle.

References

[1] ARCZYŃSKI, S., 1993. *Mechanika ruchu samochodu (Mechanics of motion of the motor vehicle)*. Warszawa: Wydawnictwo Naukowo Techniczne.

[2] CHOROMAŃSKI, W., ZBOIŃSKI, K., 1991. Optimizations of wheel-rail profiles for various condition of vehicle motion. *The Dynamics of Vehicle on Roads and on Tracks, Supplement to Vehicle System Dynamics*, 20, pp. 84-98.

[3] CHUDZIKIEWICZ, A. 1995. Study on the relation between the traveling speed and forces within the wheel/rail contact zone depending on the state of track maintenance. *Machine Dynamics Problems* 11, pp. 7-19.

[4] CROLLA, D. A., 1996. Vehicle dynamics – theory into practice. *Journal of Automobile Engineering*, 1996(210), pp. 83-94.

[5] FIRTH, G., R., 1991. *The performance of vehicle suspensions fitted with controllable dampers*. Ph. D. thesis, Department of Mechanical Engineering, The University of Leeds.

[6] GOBBI, M., LEVI, F., MASTINU, G., 2006. Multi-objective stochastic optimization of the suspension system of road vehicles. *Journal of Sound and Vibration*, 298(4), pp. 1055-1072.

[7] GOBBI, M., MASTINU, G., 2001. Analytical description and optimization of the dynamic behaviour of passively suspended vehicles. *Journal of Sound and Vibration*, 245(3), pp. 457-481.

[8] GRZYB, A., BOGACZ, R., 2015. *Wspomagana komputerowo analiza dynamiczna pojazdów szynowych (Computer-aided dynamic analysis of railway vehicles)*. Cracow University of Technology, Kraków 2015.

[9] ISO 2631–1, 1985 & 1997. *Mechanical vibration and shock. evaluation of human exposure to whole-body vibration. Part 1: General Requirements.* International Organization for Standardization.

[10] KALKER, J., J., 1982. A fast algorithm for the simplified theory of rolling contact. *Vehicle System Dynamic*s, 11(1), pp. 1-13

[11] KAMIŃSKI, E., POKORSKI, J., 1983. *Teoria samochodu. Dynamika zawieszeń i układów napędowych pojazdów samochodowych (Automobile theory. Dynamics of suspension systems and powertrains of motor vehicles).* Warszawa: WKŁ.

[12] KARDAS-CINAL, E., 2006. Investigation of ride comfort in a railway vehicle in the presence of random track irregularities. *Archives of Transport*, 18(1), pp. 5-16.

[13] KARDAS-CINAL, E., 2013. *Bezpieczeństwo i komfort jazdy pojazdu szynowego z uwzględnieniem losowych nierówności geometrycznych toru (Running safety and ride comfort of railway vehicle in the presence of random geometrical track irregularities)*. A monograph. Prace Naukowe Politechniki Warszawskiej, Transport, (94/2013), Warsaw University of Technology.

[14] KASPRZYK, T., PROCHOWSKI, L., 1990. *Teoria samochodu. Obciążenia dynamiczne zawieszeń (Automobile theory. Dynamic loads on suspension systems)*.Warszawa: WKŁ..

[15] KASPRZYK, T., PROCHOWSKI, L., SZURKOWSKI, Z., 1974. *Optymalizacja własności sprężystych i dobór konstrukcji ogumienia samochodu osobowego dla różnych warunków eksploatacji (Optimization of the spring characteristics and selection of the construction of passenger car tyres for different operation conditions). Part I: Technika Motoryzacyjna*, 10, pp. 10-12, *Part II: Technika Motoryzacyjna*, 11, pp. 14-19.

[16] KIM, T. S., HONG, K. S., KIM, R. K., PARK, J. W., HUH, C. D., 2007. Modified sensitivity control of a semi-active suspension system with MR-damper for ride comfort improvement. *Journal of the KSME (A)*, 31(1), pp. 129-138.

[17] KISILOWSKI, J. (ed), 1991. *Dynamika układu mechanicznego pojazd szynowy – tor (Dynamics of the railway vehicle-track mechanical system)*. Warszawa: PWN.

[18] KONIECZNY, J., 2011. Laboratory tests of active suspension system. *Journal of KONES Powertrain and Transport*, 18(1), pp. 263-272.

[19] KWARCIŃSKI, T., 2007. Sprawiedliwość czy efektywność? Analiza wykorzystująca ekonometryczny model wzrostu gospodarczego z historycznie optymalnym zróżnicowaniem płac (Justice or efficiency? Analysis using an econometric model of economic growth with historically optimal diversity of wages). *Acta Universitatis Lodziensis, Folia Oeconomica*, 213, 109-124.

[20] LI, H., GOODALL, R., M., 1999. Linear and non-linear skyhook damping control laws for active railway suspensions. *Control Engineering Practice*, 7, pp. 843-850.

[21] LIANG, T. Y., WANG, Z. D., TANG, M. X., ZHANG, W.L., 2012. Study on semi-active secondary suspension of railway vehicle. *Proceedings 2011 International Conference on Transportation, Mechanical, and Electrical Engineering (TMEE 2011), Institute of Electrical and Electronics Engineers (IEEE)*, pp. 1269-1272.

[22] LOZIA, Z., 1985. *Wybrane zagadnienia symulacji cyfrowej procesu hamowania samochodu dwuosiowego na nierównej nawierzchni drogi (Selected problems of digital simulation of the process of braking a two-axle motor vehicle on uneven road surface).* Phd Thesis, Warsaw University of Technology, Faculty of Automotive and Construction Machinery Engineering.

[23] LOZIA, Z., 2016. The use of a linear quarter-car model to optimize the damping in a passive automotive suspension system – a follow-on from many authors' works of the recent 40 years. *The Archives of Automotive Engineering – Archiwum Motoryzacji*, 71(1), pp. 33-65.

[24] MEIROVITCH, L. 1975. *Elements of vibration analysis*. McGraw-Hill Kogakusha.
[25] MITSCHKE, M., 1977. *Teoria samochodu. Dynamika samochodu (Automobile theory. Dynamics of motor vehicles)*. Warszawa: WKŁ.
[26] MITSCHKE, M., 1989. *Dynamika samochodu (Motor vehicle dynamics)*. Vol. 2: *Drgania (Vibrations)*. Warszawa: WKŁ.
[27] MULUKA, V., 1998. *Optimal suspension damping and axle vibration absorber for reduction of dynamic tire loads.* M. of A. Sc. thesis. Concordia University, The Department of Mechanical Engineering. Montreal, Quebec, Canada.
[28] NEWLAND, D. E., 1984: *An introduction to random vibrations and spectral analysis*. 2nd edition. Longman.
[29] O'BRIEN, E. J., CATHAL, B., PARAIC, Q., 2015. Determination of vertical alignment of track using accelerometer readings. *IMechE Stephenson Conference for Railways: Research for Railways*, pp. 21-23.
[30] ORE B176, 1989. *Bogies with steered or steering wheelsets, RP1, Utrecht, Netherlands.*
[31] ORVNÄS, A., 2010. Methods for reducing vertical carbody vibration of a rail vehicle. A literature survey. *Report in Railway Technology*, Sweden: Stockholm.
[32] ORVNÄS, A., 2011. *On active secondary suspension in rail vehicles to improve ride comfort.* Doctoral Thesis in Railway Technology. KTH, Stockholm, Sweden.
[33] OSIECKI, J., 1979. *Podstawy analizy drgań mechanicznych (Fundamentals of the analysis of mechanical vibrations)*. Kielce University of Technology, Kielce.
[34] OSIECKI, J., 1994. *Dynamika maszyn (Machinery dynamics)*. Military University of Technology, Warszawa.
[35] OSIECKI, J., GROMADOWSKI, T., STĘPIŃSKI, B., 2006. *Badania pojazdów samochodowych i ich zespołów na symulacyjnych stanowiskach badawczych (Testing of automotive vehicles and their components on simulation test stands)*. Radom-Warszawa: Wydawnictwo Instytutu Technologii Eksploatacji – PIB (Publishing House of the Institute for Sustainable Technologies – National Research Institute),
[36] PATIL, S. A., JOSHI, S. G., 2014. Experimental analysis of 2 DOF quarter-car passive and hydraulic active suspension systems for ride comfort. *Systems Science & Control Engineering: An Open Access Journal*, 2, pp. 621–631.
[37] PIOTROWSKI, J., 1990. *Poprzeczne oddziaływanie między pojazdem i torem – podstawy modelowania numerycznego (Lateral vehicle-track interaction – fundamentals of numerical modelling). Prace Naukowe Politechniki Warszawskiej, Mechanika, 118.* Warsaw University of Technology, Warszawa.
[38] ROTENBERG, R. W., 1974. *Zawieszenie samochodu (Automobile suspension system).* Warszawa: WKŁ.
[39] RYBA, D., 1974. Improvements of dynamic characteristics of automobile suspension systems (Part I. Two-mass systems). *Vehicle System Dynamics*, 3, pp. 17-46.
[40] SEKULIĆ, D., DEVIDOVIĆ, V., 2011. The effect of stiffness and damping of the suspension system elements on the optimization of the vibrational behavior of a bus. *International Journal for Traffic and Transport Engineering*, 1(4), pp. 231-244.
[41] SHARP, R. S., CROLLA, D. A., 1987. Road vehicle suspension system design – a review. *Vehicle System Dynamics*, 16, pp. 167-192.
[42] SHARP, R. S., HASSAN, S. A., 1986. An evaluation of passive automotive suspension systems with variable stiffness and damping parameters. *Vehicle System Dynamics*, 15, pp. 335-350.
[43] SIM, K. S., PARK, T. W., KIM, W. H., LEE, J. H., 2013. A study on ride improvement of a high speed train using skyhook control. *3rd International Conference on Mechanical, Production and Automobile Engineering (ICMPAE'2013) January 4-5, 2013 Bali (Indonesia).*
[44] ŚLASKI, G., 2012. *Studium projektowania zawieszeń samochodowych o zmiennym tłumieniu (A study on designing variable-damping automotive suspension systems)*. Poznań: Wydawnictwo Politechniki Poznańskiej, Series "Dissertations", 481.
[45] VERROS, G., NATSIAVAS, S., PAPADIMITRIOU, C., 2005. Design optimization of quarter-car models with passive

and semi-active suspensions under random excitation. *Journal of Vibration and Control*, 11, pp. 581-606.

[46] WICKENS, A., 1976. Steering and dynamic stability of railway vehicles. *Vehicle System Dynamics: International Journal of Vehicle Mechanics and Mobility*, 5(1-2), pp. 15-46.

[47] WONG, J. Y., 2001.: *Theory of ground vehicles*. Canada-USA: John Wiley & Sons, Inc.

[48] YI, K. S., SONG, B. S., 1999. Observer design for semi-active suspension control. *Vehicle System Dynamics*, 32, pp. 129-148.

[49] ZBOIŃSKI, K., 2000. Metodyka modelowania dynamiki pojazdów szynowych z uwzględnieniem zadanego ruchu unoszenia i jej zastosowania (Methodology of modelling the railway vehicle dynamics with taking into account a predefined reference frame motion; applications of the methodology). *Prace Naukowe Politechniki Warszawskiej, Transport*, 43, pp. 3-213.

[50] ZBOIŃSKI, K., 2004. Numerical and traditional modelling of dynamics of multi-body system in type of a railway vehicle. *Archives of Transport*, 16(3), 2004, pp. 82-106.

[51] ZHOU, J., GOODALL, R., REN, L., ZHANG, H., 2009. Influences of car body vertical flexibility on ride quality of passenger railway vehicles. *Proceedings of the Institution of Mechanical Engineers, Part F: Journal of Rail and Rapid Transit*, 223(5), pp. 461-471.